ANTIOXIDANTS & REDOX SIGNALING
Volume 17, Number 5, 2012

DOI: 10.1089/ars.2011.4398

ORIGINAL RESEARCH COMMUNICATION

Peroxynitrite Mediates Disruption of Ca^{2+} Homeostasis by Carbon Monoxide *via* Ca^{2+} ATPase Degradation

Nishani T. Hettiarachchi,[1,*] John P. Boyle,[1,*] Claudia C. Bauer,[1] Mark L. Dallas,[1] Hugh A. Pearson,[2] Shuichi Hara,[3] Nikita Gamper,[2] and Chris Peers[1]

Abstract

Aim: Sublethal carbon monoxide poisoning causes prolonged neurological damage involving oxidative stress. Given the central role of Ca^{2+} homeostasis and its vulnerability to stress, we investigated whether CO disrupts neuronal Ca^{2+} homeostasis. ***Results:*** Cytosolic Ca^{2+} transients evoked by muscarine in SH-SY5Y cells were prolonged by CO (applied via the donor CORM-2), and capacitative Ca^{2+} entry (CCE) was dramatically enhanced. Ca^{2+} store mobilization by cyclopiazonic acid was similarly augmented, as was the subsequent CCE, and that evoked by thapsigargin. Ca^{2+} rises evoked by depolarization were also enhanced by CO, and Ca^{2+} levels often did not recover in its presence. CO increased intracellular nitric oxide (NO) and all effects of CO were prevented by inhibiting NO formation. However, NO donors did not mimic the effects of CO. The antioxidant ascorbic acid inhibited effects of CO on Ca^{2+} signaling, as did the peroxynitrite scavenger, FeTPPS, and CO increased peroxynitrite formation. Finally, CO caused significant loss of plasma membrane Ca^{2+}ATPase (PMCA) protein, detected by Western blot, and this was also observed in brain tissue of rats exposed to CO *in vivo*. ***Innovation:*** The cellular basis of CO-induced neurotoxicity is currently unknown. Our findings provide the first data to suggest signaling pathways through which CO causes neurological damage, thereby opening up potential targets for therapeutic intervention. ***Conclusion:*** CO stimulates formation of NO and reactive oxygen species which, via peroxynitrite formation, inhibit Ca^{2+} extrusion via PMCA, leading to disruption of Ca^{2+} signaling. We propose this contributes to the neurological damage associated with CO toxicity. *Antioxid. Redox Signal.* 17, 744—755.

Introduction

Carbon monoxide (CO) is currently receiving attention as an important intracellular signaling molecule and potential therapeutic agent (10, 29, 36). However, it is better established as a potent toxin generated by incomplete hydrocarbon combustion (*e.g.,* from motor exhaust fumes, gas appliances, and tobacco smoke). CO poisoning accounts for more than 50% of all fatal poisonings (7, 25), and acute, sublethal exposures lead to significant numbers of hospital admissions (22). Although the number of fatalities arising from acute exposure are relatively low compared with, For example, heart disease or cancer, chronic exposure commonly produces neurological and cardiovascular damage (8, 32, 48), particularly in the aging population, and symptoms are difficult to diagnose (17). An estimated 10% of patients treated for CO poisoning are left with prolonged neurological damage (9, 22).

Despite this awareness, little detail of the mechanisms underlying CO toxicity is known. The original proposal that CO is toxic through hypoxemia via its binding to hemoglobin (14) is now considered unlikely as a sole explanation, since many features of CO toxicity are not observed following hypoxic/ischemic damage (42). Instead, mechanisms that also account for physiological (signaling) actions of CO are being considered as possible toxicity mechanisms. For example, CO can stimulate increased reactive oxygen species (ROS) primarily from mitochondria (3, 31, 50). This may be protective—a form of "oxidative preconditioning" (3, 47)—but could be deleterious by promoting oxidative stress. CO can also stimulate NO production, possibly by activating nitric oxide synthase (19, 21). Production of both ROS and NO by CO can also increase oxidative/nitrosative stress through formation of peroxynitrite [$ONOO^-$; (15)]. Oxidative stress can cause neurodegeneration via disruption of Ca^{2+} homeostasis, a process

Leeds Institute of Genetics, Health & Therapeutics, Faculties of [1]Medicine and Health and [2]Biological Sciences, University of Leeds, Leeds, United Kingdom.
[3]Department of Forensic Medicine, Tokyo Medical University, Tokyo, Japan.
*These authors contributed equally to this study.

Innovation

Although carbon monoxide (CO) is currently under intense investigation as a major intracellular signaling molecule, it is better established as a highly toxic agent. However, very little is known of the mechanisms underlying its neurotoxicity. The present study shows for the first time that acute CO exposure causes major disruption to neuronal Ca^{2+} homeostasis. This deleterious action arises from the ability of CO to stimulate increased production of both reactive oxygen species and nitric oxide. These agents combine to form peroxynitrite which leads to damage/degradation of the plasmalemmal Ca^{2+} ATPase (PMCA), a key protein required for control of Ca^{2+} homeostasis. Loss of PMCA was also observed in rat brain samples following inhalation of CO at sublethal levels. These finds reveal for the first time a key homeostatic protein targeted for destruction by toxic levels of CO, and identify the underlying mechanism leading to PMCA degradation. Through identification of the underlying mechanisms, our study reveals potential pathways which may provide therapeutic targets to combat the neurological damage associated with CO toxicity.

implicated in aging and neurodegenerative diseases such as Alzheimer's disease (11, 23, 24). For example, apoptosis can arise from Ca^{2+}-dependent activation of caspases, and the rise of $[Ca^{2+}]_i$ can occur through oxidative triggering of Ca^{2+} influx and/or disruption of Ca^{2+} buffering / extrusion (2, 11, 20, 24). We have examined the effects of CO on neuronal Ca^{2+} signaling using the human neuroblastoma, SH-SY5Y, a line used extensively for studying Ca^{2+} homeostasis and neuronal signaling (18, 33—35, 46). We reveal that CO stimulates formation of $ONOO^-$ and thereby disrupts Ca^{2+} signaling via plasma membrane Ca^{2+} ATPase downregulation. Such effects, confirmed in brain tissue of rats exposed to CO *in vivo,* may contribute to the neurological damage associated with CO poisoning.

Results

Effects of CO on Ca^{2+} signaling

Activation of M_3 muscarinic receptors in SH-SY5Y cells triggers release of Ca^{2+} from intracellular stores following generation of inositol trisphosphate (IP_3) which in turn activates store-depletion mediated (capacitative) Ca^{2+} entry [CCE; (6, 30, 39, 40)]. These events can be resolved temporally by exposing cells to muscarine (100 μM) in the absence of extracellular Ca^{2+} (replaced with 1m*M* EGTA). This evoked a rise of $[Ca^{2+}]_i$ due to mobilization from intracellular stores. Following removal of muscarine, restoring Ca^{2+} to the extracellular solution causes a second rise of $[Ca^{2+}]_i$ resulting from CCE (Fig. 1A). The effects of the CO donor, CORM-2, on these responses are illustrated in Figures 1A and B. In the presence of CORM-2 (30 μM), two striking differences were noted: first, the transient rise of $[Ca^{2+}]_i$ evoked by muscarine in the absence of extracellular Ca^{2+} decayed much more slowly, as highlighted in Figure 1B (quantified as transient integral and $t_{1/2}$ in Fig. 1C). Second, CCE observed when Ca^{2+} was restored to the perfusate following washout of muscarine was dramatically enhanced (Figs. 1A and 1C). None of these parameters was significantly altered by iCORM (30 μM), the inactive form of CORM-2 which does not release CO (hatched bars, Fig. 1C). CORM-2 was applied in this and all subsequent figures for 3 min before additional experimental manoeuvres, and present throughout. At 30 m*M*, CORM-2 led to a CO concentration of 33 μM in solution.

Depolarization of SH-SY5Y cells by exposure to 50 m*M* K^+ causes a rapid rise of $[Ca^{2+}]_i$ due to Ca^{2+} influx through L- and N-type Ca^{2+} channels (28, 35) as shown in Figures 2A and 2B. At 3 μM, CORM-2 did not significantly alter the amplitude of high K^+-induced rises of $[Ca^{2+}]_i$. However, at 10 μM, CORM-2-evoked rises of $[Ca^{2+}]_i$ were not significantly altered in amplitude in most recordings, but in 12 out of 27 recordings, $[Ca^{2+}]_i$ rose dramatically during the exposure to high K^+, and did not recover. In the presence of 30 μM CORM-2, the majority of recordings (24 out of 26) revealed this apparently uncontrolled rise of $[Ca^{2+}]_i$. Such effects of CORM-2 (but not iCORM) to evoke poorly controlled rises of $[Ca^{2+}]_i$ were similar to its effects on CCE shown in Figure 1A. It was possible that these effects arose from increased voltage-gated Ca^{2+} entry on depolarization. To address this, we measured Ca^{2+} currents directly, as previously described (28, 35). Surprisingly, Ca^{2+} currents were significantly ($p < 0.001$, $n = 6$) inhibited by CORM-2 (30 μM), as shown in Figure 2C. Currents were significantly reduced by CORM-2 over the voltage range −20mV to +40mV ($p < 0.05$—$p < 0.001$, paired *t*-tests).

To investigate disruption of M_3 receptor-mediated signaling further, we depleted stores directly with cyclopiazonic acid (CPA, which reversibly inhibits the endoplasmic reticulum (ER) Ca^{2+} ATPase). In the absence of extracellular Ca^{2+}, CPA (10 μM) evoked transient rises of $[Ca^{2+}]_i$ in control cells and, following its removal, restoration of Ca^{2+} to the perfusate evoked a rise of $[Ca^{2+}]_i$ due to CCE (Fig. 3A). In the presence of CORM-2, both the CPA-evoked transient rise of $[Ca^{2+}]_i$ and the resultant CCE were dramatically augmented (Fig. 3A), suggesting CO acts downstream of receptor activation and coupling to stores. Store depletion using thapsigargin (TG; applied for 20 min prior to monitoring $[Ca^{2+}]_i$) evoked larger CCE than was seen following CPA treatment (likely due to more complete store emptying), which was further enhanced by CORM-2, but not (at least at lower concentrations) by iCORM, again suggesting that CO augmented CCE in these cells (Fig. 3B).

These effects of CO likely represent the cellular consequences of toxic CO exposure. To distinguish these effects from those arising from increased endogenous CO production, we investigated the effects of HO-1 induction by exposing cells to hemin (100 μM for 24 h). Such treatment caused a marked induction of HO-1, but was without significant effect on muscarine-evoked Ca^{2+} signals (Supplementary Fig. 1; supplementary data are available online at www.liebertonline.com/ars).

NO-dependence of CO disruption of Ca^{2+} signaling

Multiple intracellular signaling pathways are modulated by CO, including those involving mitochondria and NO. To examine whether the effects of CO arose due to mitochondrial inhibition, we compared its effects with those of the mitochondrial inhibitor antimycin A. As shown in Supplementary Figure 2, antimycin A (3 μg/ml) increased the decay time and

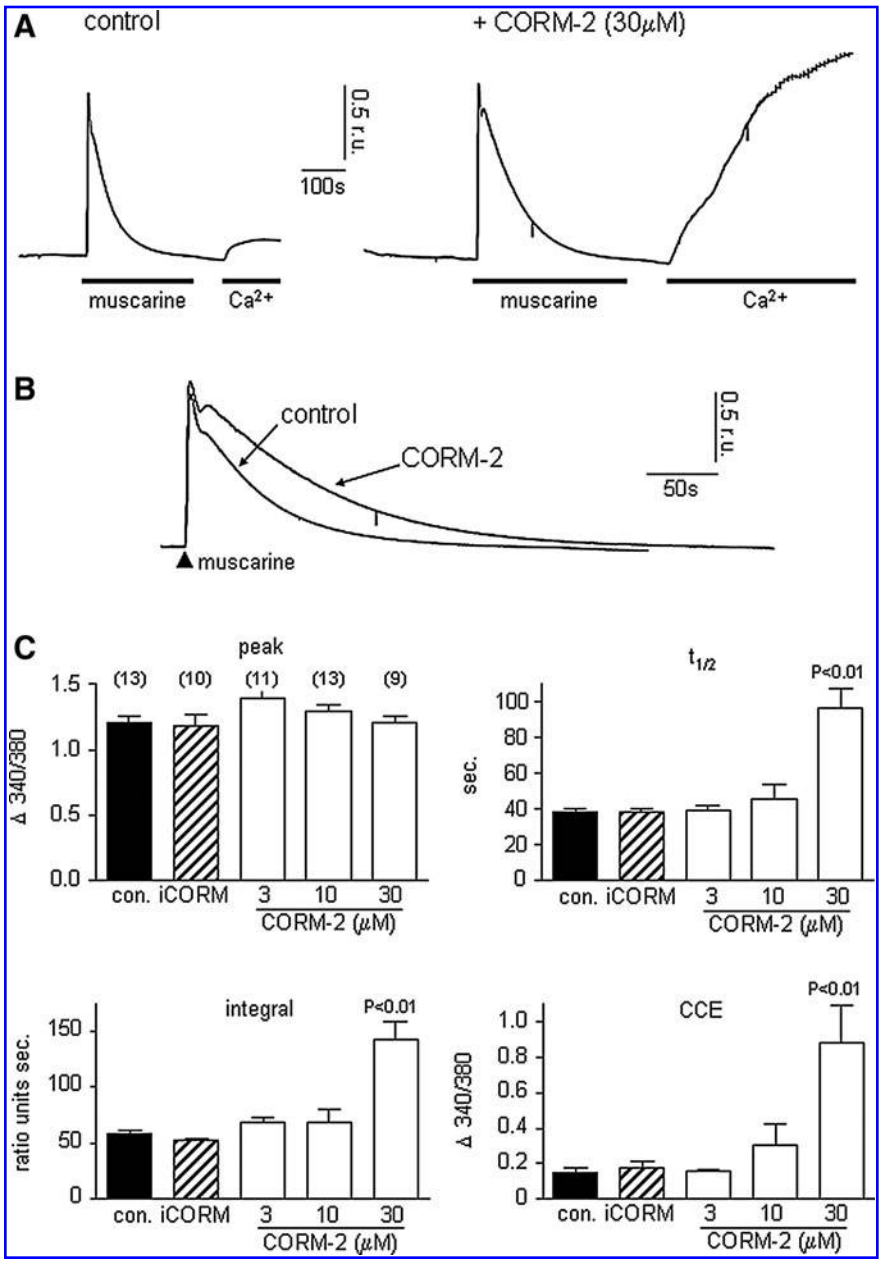

FIG. 1. CO disrupts muscarine-evoked Ca^{2+} signaling in SH-SY5Y cells. (A) Representative recordings of $[Ca^{2+}]_i$ made in SH-SY5Y cells in the absence (control, *left*) or presence (*right*) of 30 μM CORM-2. In both cases, Ca^{2+} was initially absent from the perfusate (replaced with 1 m*M* EGTA), and for the periods indicated by the *horizontal bars*, cells were exposed to 100 μM muscarine. Following washout of muscarine, Ca^{2+} (2.5 m*M*) was readmitted to the perfusate and CCE determined. **(B)** The transient rises of $[Ca^{2+}]_i$ evoked by muscarine shown in **(A)** are superimposed to highlight the prolonged nature of the response in the presence of CORM-2. **(C)** Mean responses to 100 μM muscarine evoked in the absence of other drugs (control, *solid bars*) in the presence of the control compound, iCORM (30 μM; *hatched bars*) or in the presence of 3–30 μM CORM-2 (*open bars*). Traces such as are shown in **(A)** were measured for peak response (peak), the time taken for responses to fall to 50% of their peak value ($t_{1/2}$), and responses were also integrated (integral). The amplitudes of the CCE responses are also shown. In each case, *bars* represent means ± s.e.m., taken from the number of recordings indicated above each bar. *P* values indicate significant differences from controls.

integral of the muscarine-evoked response (similar to the effects of CO). However, it also significantly raised basal Ca^{2+} levels and almost fully suppressed CCE. These latter effects clearly distinguish the effects of CO from those of direct mitochondrial inhibition.

To investigate whether NO mediated the effects of CO described in Figures 1–3, we examined whether the NOS inhibitor , L-NAME, could interfere with the actions of CO. Figure 4A shows that L-NAME (1 m*M*, applied for 1 h prior to, and during experiments) fully reversed the augmenting effects of CO on muscarine-evoked rises of $[Ca^{2+}]_i$ and the subsequent CCE. Similarly, the dramatic rises of $[Ca^{2+}]_i$ evoked by exposure of cells to 50 m*M* K^+-containing solutions were reduced to levels seen in cells not exposed to CO (Fig. 4B). These findings (and also the observation that CO augmentation of TG-evoked CCE was prevented in the presence of L-NAME, see Fig. 5C), suggest that CO modulates Ca^{2+} homeostasis via production of NO. In confirmation of this idea, we found that CORM-2 increased fluorescence of the NO-sensitive fluoroprobe, DAF-2 (Fig. 4C). Importantly, this increased fluorescence, indicative of increased NO, was not observed when cells were exposed to iCORM, and was prevented in the presence of L-NAME (Fig. 4C). Thus, CO appears to modulate Ca^{2+} homeostasis via its ability to stimulate NO production. Such a conclusion would predict that exposure of cells to NO, or NO donor compounds, would mimic the effects of CO. However, S-nitroso N-acetylpenicillamine (SNAP; 10 or 100 μM) was unable to alter significantly the muscarinic-receptor mediated Ca^{2+} signaling (Fig. 5A), or rises of $[Ca^{2+}]_i$ evoked by 50 m*M* K^+ (Fig. 5B). Similarly, although L-NAME prevented the augmentation of CCE seen in the presence of CO (Fig. 4), SNAP did not alter CCE (Fig. 5C). A similar lack of effect was seen with three other NO donors (Supplementary Table 1). Thus, although

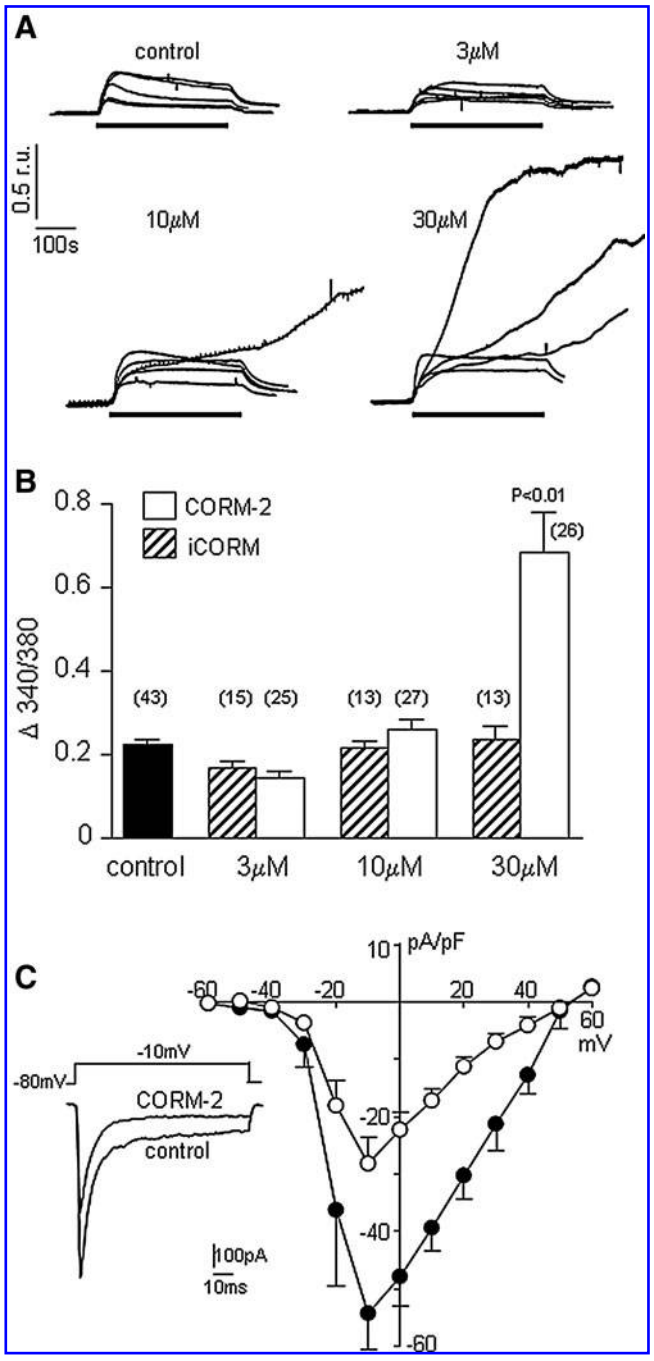

FIG. 2. CO enhances rises of $[Ca^{2+}]_i$ evoked by depolarization, yet inhibits voltage-gated Ca^{2+} currents. (A) Representative recordings of $[Ca^{2+}]_i$ made in control cells and cells exposed to 3–30 μM CORM-2, as indicated. For the periods indicated by the *bar* in each case, cells were exposed to perfusate containing 50 m*M* K^+. **(B)** Mean (±s.e.m.) rises of $[Ca^{2+}]_i$ evoked by 50 m*M* K^+ in control cells (*solid bar*) or 3–30 μM of either iCORM (*hatched bars*) or CORM-2 (*open bars*). The number of recordings averaged are indicated above each bar. *P* value indicates significant difference from control. **(C)** *Left*, example of whole-cell Ca^{2+} channel currents evoked in a SH-SY5Y cell before and during exposure to 30 μM CORM-2. *Right*, mean (±s.e.m.) Ca^{2+} current density versus voltage plot determined in 6 cells before and during exposure to 30 μM CORM-2. Currents were significantly reduced by CORM-2 over the voltage range −20mV to +40mV ($p < 0.05$—$p < 0.001$, paired *t*-tests).

effects of CO were NO-dependent, NO alone was unable to mimic the actions of CO.

Involvement of peroxynitrite formation on CO modulation of Ca^{2+} signaling

Since CO also increases ROS production, we investigated the possible role of ROS in the ability of CO to modulate Ca^{2+} signaling in SH-SY5Y cells. As illustrated in Figure 6A, the CO-induced increases in decay time and integral transient of the rise of $[Ca^{2+}]_i$ evoked by muscarine mobilization from internal stores was completely reversed in the presence of the antioxidant ascorbic acid (200 μM). Similarly, the augmentation by CO of CCE observed following muscarine exposure and removal (Fig. 6A) and the CCE observed following TG treatment (Fig. 6B), were fully reversed by ascorbic acid. Finally, the effects of CO on 50 m*M* K^+ evoked rises of $[Ca^{2+}]_i$ were also fully prevented by ascorbic acid (Fig. 6C).

The observations that the effects of CO depended both on NO and on ROS production (Figs. 4 and 6) suggested to us the involvement of peroxynitrite ($ONOO^-$) formation, since this is rapidly formed from NO and the ROS superoxide ($O_2^{\cdot-}$). To investigate this, we examined whether CO could evoke $ONOO^-$ production, using the $ONOO^-$ -sensitive fluoroprobe, APF (38). APF fluorescence increased in SH-SY5Y cells in response to CORM-2 (10 and 30 μM), but the increases seen in response to iCORM were not significantly different from the slight upward drift in fluorescence observed with time (Figs. 7A and 7B). Importantly, increased APF fluorescence was prevented in the presence of ascorbic acid or L-NAME, supporting the idea that APF is indeed reporting increased $ONOO^-$ levels in response to CO and, hence, that $ONOO^-$ may mediate the effects of CO on Ca^{2+} signaling. To test this further, we investigated the effects of the $ONOO^-$ decomposition catalyst, FeTPPs (5,10,15,20-tetrakis-[4-sulfonatophenyl]-porphyrinato-iron[III]; 50 μM), which rapidly converts $ONOO^-$ to nitrate (27). As illustrated and quantified in Figure 8, FeTPPs effectively reversed the effects of CO on muscarine-evoked rises of $[Ca^{2+}]_i$ and subsequent CCE (Fig. 8A) and rises of $[Ca^{2+}]_i$ evoked by 50 m*M* K^+ (Fig. 8B).

A role for the plasmalemmal Ca^{2+} ATPase in mediating the effects of CO

Our findings thus far indicated that CO disrupted all aspects of evoked Ca^{2+} signaling investigated, raising the possibility that it may act via disruption of the ability of cells to regulate or control rises of $[Ca^{2+}]_i$ regardless of the source of Ca^{2+} rise. Given the known susceptibility of the plasma membrane Ca^{2+}-ATPase (PMCA) to oxidative stress (13), we investigated the effects of CO on PMCA levels using a pan anti-PMCA antibody. Exposure of cells to CORM-2 (but not iCORM) for 20 min caused a significant reduction in protein levels, regardless of the presence of muscarine (Figs. 9A and 9C). This reduction in PMCA protein levels was recovered separately either by ascorbic acid (200 μM) or L-NAME (1 m*M*; Figs. 9B and 9C). These data strongly suggest that the disruption of Ca^{2+} signaling caused by CO may be attributed to the $ONOO^-$-dependent loss of PMCA.

To investigate whether a similar degradation of PMCA occurred as a result of CO poisoning *in vivo*, we used the same antibody to probe whole-brain homogenates of rats exposed to either 1000 or 3000 ppm CO for 40 min. As shown in Figures

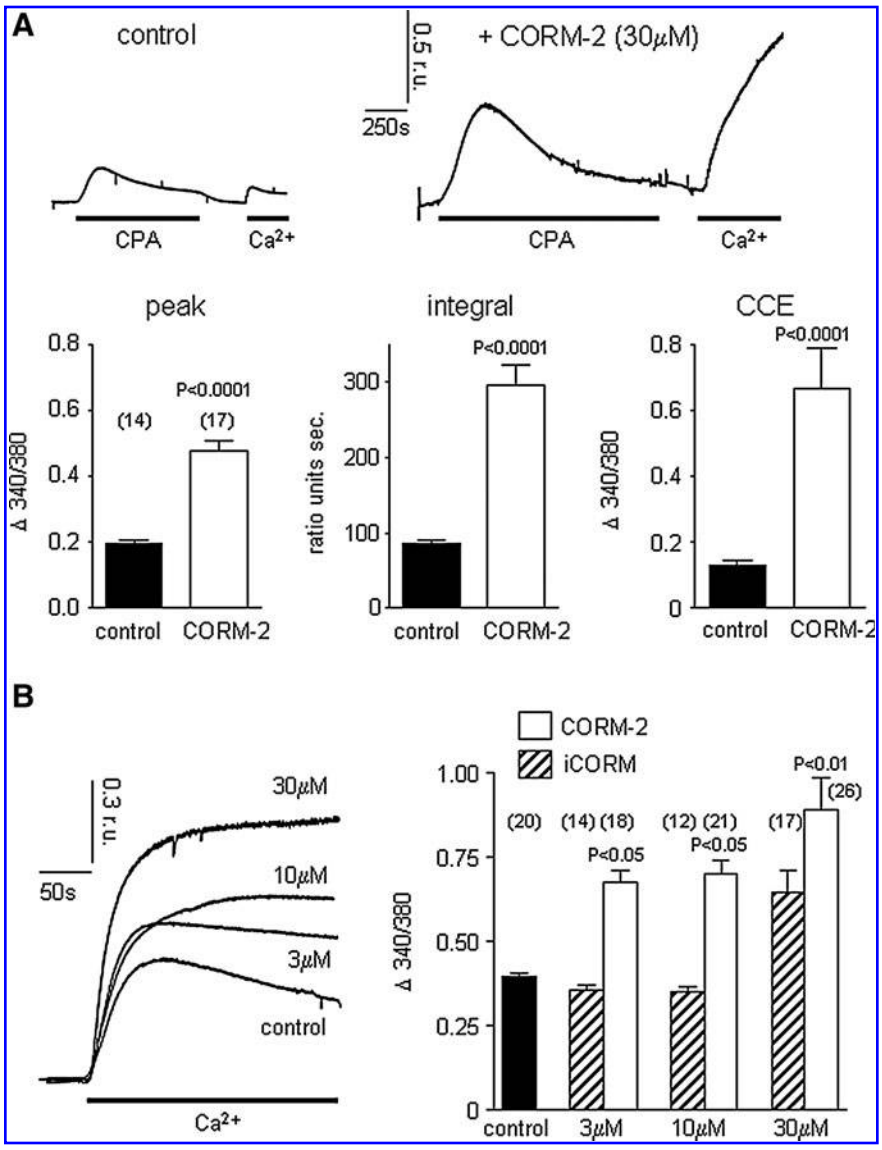

FIG. 3. CO augments store-depletion mediated Ca^{2+} entry. (A) Representative recordings of $[Ca^{2+}]_i$ made in SH-SY5Y cells in the absence (control, *left*) or presence (*right*) of 30 μM CORM-2. In both cases, Ca^{2+} was initially absent from the perfusate (replaced with 1 m*M* EGTA), and for the periods indicated by the *horizontal bars*, cells were exposed to 10 μM cyclopiazonic acid (CPA). Following washout of CPA, Ca^{2+} was readmitted to the perfusate and CCE determined. *Below,* mean peak and integral of responses to 10 μM CPA, and mean CCE are plotted. In each case, *bars* represent means ± s.e.m., taken from the number of recordings indicated above each bar. *P* values indicate significant differences from controls. **(B)** *Left*, representative traces of capacitative Ca^{2+} entry (CCE) measured in cells in the absence (control) or presence of 3—30 μM CORM-2. Cells were previously exposed to 1 μM thapsigargin for 20 min in the absence of extracellular Ca^{2+} (replaced with 1 m*M* EGTA). Following this, Ca^{2+} (2.5 m*M*) was readmitted to the perfusate for the period indicated by the *horizontal bar*. *Right,* mean (± s.e.m.) peak CCE responses measured in control cells (*solid bar*) or 3–30 μM of either iCORM (*hatched bars*) or CORM-2 (*open bars*). The number of recordings averaged are indicated above each bar. *P* values for significance are also indicated.

10A and 10B, a concentration-dependent loss of this important regulator of $[Ca^{2+}]_i$ was observed, indicating that our findings in SH-SY5Y cells reflect the neurotoxic effects of CO *in vivo*.

Discussion

Amid the widespread and developing interests in CO as a significant physiological signaling molecule and therapeutic agent, it is easy to lose sight of the fact that it is also a highly toxic gas. Exposure to toxic levels of CO can, when not lethal, cause delayed neurological/neuropsychiatric symptoms (26, 31, 32). At the cellular level, toxic levels of CO can cause apoptosis and necrosis, and toxicity has been attributed to oxidative damage. Although most cellular studies have employed non-neuronal tissue, such as endothelial cells (43, 45), one recent study has examined the toxic effects of CO inhalation on hippocampal neurons and, consistent with studies in endothelial cells, indicates that neuronal injury and death caused by CO arises from oxidative damage leading to apoptosis (12). Despite the known association of oxidative stress with disturbances of Ca^{2+} homeostasis that can lead to neuronal damage as observed in aging brain samples and those obtained from sufferers of neurodegenerative disorders (11, 24), the possibility that CO might perturb neuronal Ca^{2+} homeostasis has not been studied in depth.

The present study indicates that CO acts to modulate multiple aspects of Ca^{2+} signaling in human neuroblastoma SH-SY5Y cells. Thus, CO modified Ca^{2+} mobilization from intracellular stores (Figs. 1 and 3), store depletion-mediated (capacitative) Ca^{2+} entry (Figs. 1 and 3) and voltage-gated Ca^{2+} entry (Fig. 2). Our results further indicate that CO acts in this manner via $ONOO^-$ formation arising from increased levels of both NO and ROS (Figs. 4, 6–8). The involvement of NO is indicated by the observations that L-NAME prevents the effects of CO to disrupt Ca^{2+} signaling, and that CO leads to increased levels of NO, as monitored fluorimetrically (Fig. 4). Our findings agree with previous studies suggesting that CO can stimulate NO formation in other systems (19, 21) and support a previous conclusion that CO neurotoxicity

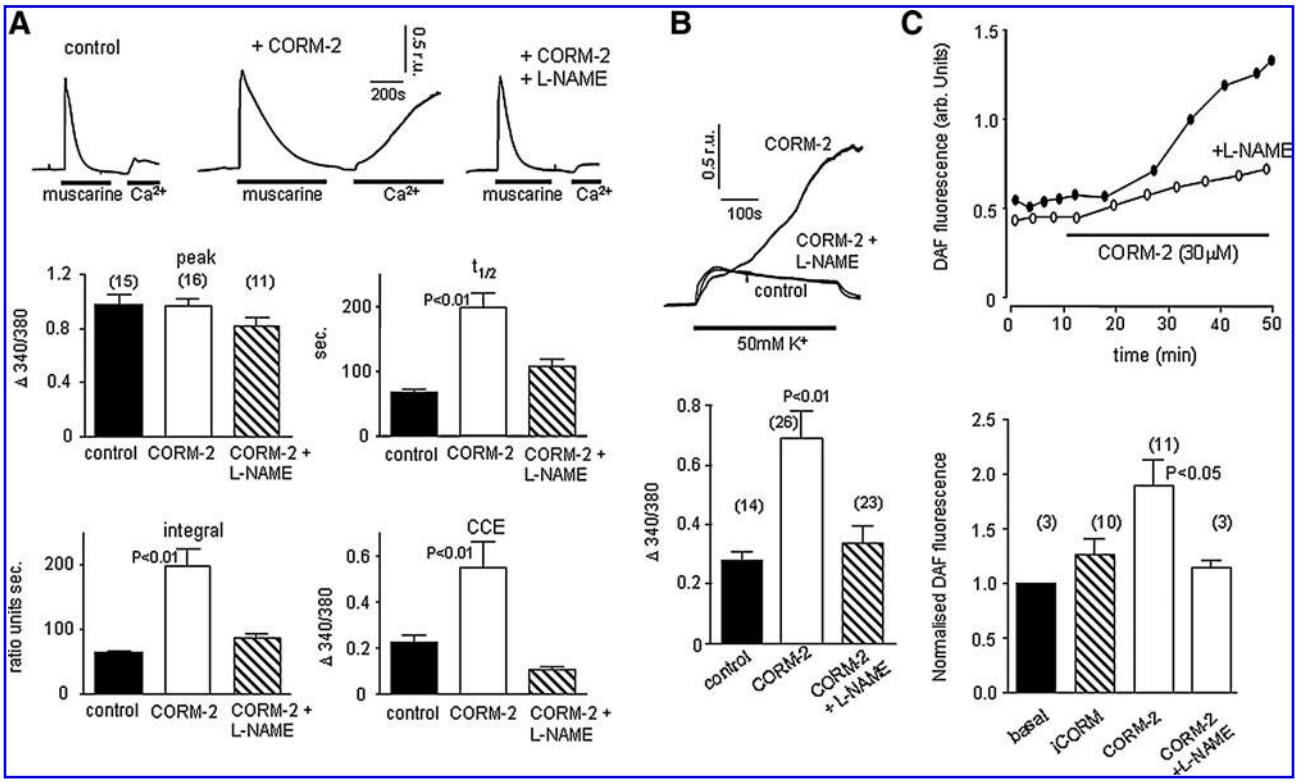

FIG. 4. Disruption of Ca^{2+} homeostasis by CO is dependent on NO formation. (A) Representative recordings of $[Ca^{2+}]_i$ made in SH-SY5Y cells in the absence (control, *left*) or presence (*middle*) of 30 μM CORM-2, and in the presence of both 30 μM CORM-2 and 1 m*M* L-NAME (*right*). In each case, Ca^{2+} was initially absent from the perfusate (replaced with 1 m*M* EGTA), and for the periods indicated by the *horizontal bars*, cells were exposed to 100 m*M* muscarine. Following washout of muscarine, Ca^{2+} was readmitted to the perfusate as indicated and CCE determined. *Bar graphs* plot mean responses to 100 m*M* muscarine evoked in the absence of other drugs (*solid bars*) in the presence of CORM-2 (30 μM; *open bars*) or in the presence of 30 μM CORM-2 and 1 m*M* L-NAME (*hatched bars*). Traces such as the ones shown above were measured for peak response (peak), the time taken for responses to fall to 50% of their peak value ($t_{1/2}$), and responses were also integrated (integral). The amplitudes of the CCE responses are also shown. In each case, *bars* represent means ± s.e.m., taken from the number of recordings indicated above each bar. *P* values indicate significant differences from controls. **(B)** *Upper*, representative recordings of $[Ca^{2+}]_i$ made in control cells, cells exposed to 30 μM CORM-2, and in the presence of both 30 μM CORM-2 and 1 m*M* L-NAME) as indicated. For the periods indicated by the *bar*, cells were exposed to perfusate containing 50 m*M* K^+. *Lower*, mean (± s.e.m.) rises of $[Ca^{2+}]_i$ evoked by 50 m*M* K^+ in control cells (*solid bar*), 30 μM CORM-2 (*open bar*) and in the presence of both 30 μM CORM-2 and 1 m*M* L-NAME (*hatched bar*). The number of recordings averaged are indicated above each bar. *P* values indicate significant differences from controls. **(C)** *Upper*; example measurements of DAF fluorescence sampled every 2–5 min in SH-SY5Y cells. For the period indicted by the *horizontal bar*, cells were exposed to 30 μM CORM-2 alone (*solid symbols*) or 30 μM CORM-2 in the presence of 1 m*M* L-NAME (*open symbols*). *Lower*, mean (± s.e.m.) rises of DAF fluorescence evoked in the absence of drugs (*solid bar*), in the presence of 30 μM iCORM (*hatched bar*) or in the presence of 30 μM CORM-2 or both 30 μM CORM-2 and 1 m*M* L-NAME (*open bars*). The number of recordings averaged are indicated above each bar. *P* values indicate significant differences from controls.

depends on activation of neuronal nitric oxide synthase (nNOS; (44)). Indeed, our findings provide a likely downstream effect that could account for CO neurotoxicity; the disruption of Ca^{2+} homeostasis. Importantly, however, the additional requirement of increased ROS in order to observe the effects of CO is clearly indicated by the fact that NO donors alone could not mimic effects of CO (Fig. 5, Supplementary table 1). Thus, NO formation alone is not sufficient to account for the effects of CO on Ca^{2+} homeostasis.

CO has previously been proposed to increase $ONOO^-$ formation in vascular endothelial cells, leading to the induction of apoptosis (43, 45). These studies indicated that caspase activation (indicating apoptosis initiation) could be prevented by an inhibitor of NOS, or by a $ONOO^-$ scavenger. Given these findings, and our observation that the effects of CO reported here were separately prevented by inhibition of either NO or ROS formation, we explored the potential involvement of $ONOO^-$. We first monitored production of $ONOO^-$ using the fluoroprobe APF. This probe was originally produced to discriminate between ROS species, and was found to be useful in the detection of $ONOO^-$ and also hydroxyl radicals ($OH^•$) and hypochlorite (^-OCl) (38). Its ability to detect $ONOO^-$ with significant selectivity has subsequently been confirmed (*e.g.*, Ref. 37). Our finding that APF fluorescence increased in response to CO in a manner that was dependent on both NO and ROS (Fig. 7) strongly suggested this fluoroprobe is reporting increased formation of $ONOO^-$, and so we conclude that CO does indeed increase $ONOO^-$ in our cells. This conclusion was supported by the observation that the $ONOO^-$ decomposition catalyst, FeTPPs, prevented all of the effects of CO to disrupt Ca^{2+} homeostasis (Fig. 8).

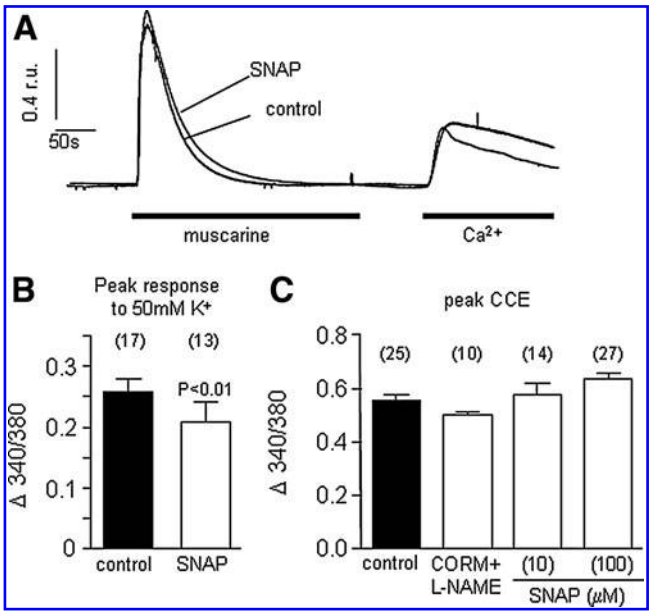

FIG. 5. NO donors do not mimic the effects of CO. (A) Superimposed representative recordings of $[Ca^{2+}]_i$ made in SH-SY5Y cells in the absence (control) or presence of the NO donor, SNAP (10 μM). Ca^{2+} was initially absent from the perfusate (replaced with 1 m*M* EGTA), and for the periods indicated by the *horizontal bars*, cells were exposed to 100 μM muscarine. Following washout of muscarine, Ca^{2+} was readmitted to the perfusate and CCE determined. **(B)** Mean (±s.e.m.) rises of $[Ca^{2+}]_i$ evoked by 50 m*M* K^+ in the absence (*solid bar*) or presence of SNAP (10 m*M*). *P* values indicate significant differences from controls. The number of recordings averaged are indicated above each bar. **(C)** Mean (±s.e.m.) peak CCE responses measured in control cells (*solid bar*), during exposure to 10 μM CORM-2 in the presence of 1 m*M* L-NAME, and in the presence of SNAP (10 or 100 μM). The number of recordings averaged are indicated above each bar. Cells were previously exposed to 1 μM thapsigargin for 20 min in the absence of extracellular Ca^{2+}(replaced with 1 m*M* EGTA).

The fact that CO modulated the rises of $[Ca^{2+}]_i$ observed following activation of diverse Ca^{2+} entry/mobilization pathways suggested that it was unlikley to modify various proteins that contribute to each of these responses individually. Instead, we reasoned that CO was more likely to act via a part of the Ca^{2+} signaling pathway common to all manouevres used to raise $[Ca^{2+}]_i$ in this study, namely the protein(s) responsible for restoring $[Ca^{2+}]_i$ to baseline levels. Once cytosolic $[Ca^{2+}]$ has increased, it is removed either via re-uptake into organelles (primarily the ER, but also mitochondria) or via extrusion into the extracellular space. We discounted ER re-uptake as a likely site of action, since when ER uptake was inhibited by CPA (Fig. 3), the ensuing rise of $[Ca^{2+}]_i$ was still augmented by CO. Instead, CO modulation of Ca^{2+} extrusion was investigated. Specifically, we investigated the possible involvement of the plasmalemmal Ca^{2+} ATPase, since a previous study suggested that $ONOO^-$ inhibits CaATPase activity in synaptosomal preparations (13). Furthermore, the Ca^{2+} ATPase is susceptible to oxidative damage/destruction (reviewed by Ref. 4). In agreement with such studies, and consistent with our functional studies, Western blots indicated that CO reduced Ca^{2+} ATPase protein levels (Fig. 9). Thus, we propose that CO disrupts Ca^{2+} signaling in SH-SY5Y cells via degradation of the plasmalemmal Ca^{2+} ATPase as a result of formation of $ONOO^-$. We further propose that this mechanism contributes to the prolonged neurological damage associated with CO toxicity, since a similar degradation of the Ca^{2+} ATPase was observed in brain tissue taken from rats previously exposed to CO acutely (Fig. 10).

The present study has revealed a deleterious aspect of the influence of CO on intracellular signaling mechanisms, which contrasts with recognized protective effects of CO against apoptosis (*e.g.*, in the endothelium (41)). Whether this is due to the fact that the present study employed neuronal tissue, whereas many previous studies have employed other tissues, is presently unknown. However, it is important to note that, whilst some of the beneficial effects of HO-1 can be mimicked by exogenous CO (for example, protection against experimental focal ischemia (49)), there are additional benefits observed following HO-1 induction (*i.e.*, increased degradation of cytotoxic heme, production of biliverdin and hence bilirubin, a powerful antioxiant), which may be neuroprotective (1) and HO-1 location will likely influence the cellular actions of endogenous CO (see Ref. 10 for review). Thus, whilst the hopes for exogenous CO therapy remain justifiably high, potentially deleterious actions, such as those reported here, must be fully considered.

Materials and Methods

Tissue culture

SH-SY5Y cells were cultured as previously described (34, 35) in a 1:1 mixture of Ham's F12 medium and Eagle's minimal essential medium, supplemented with 10% (v/v) fetal calf serum, 1% nonessential amino acids, and 0.1% gentamicin (all from GIBCO Life Sciences, Paisley, Scotland, UK). Cells were incubated at 37°C in a humidified incubator gassed with 95% air and 5% CO_2, passaged every 7 days and used for up to 14 passages.

Monitoring $[Ca^{2+}]_i$

Cells were plated onto two 10 mm glass coverslips (thickness 0) after dilution to the desired concentration with culture media. Prior to experiments, cells were incubated in HEPES-buffered saline containing 4 μM Fura-2AM (Invitrogen) at room temperature (22–24°C) and left in the dark for 40 min. HEPES-buffered saline was composed of (in m*M*): NaCl 135, KCl 5, $MgSO_4$ 1.2, $CaCl_2$ 2.5, HEPES 5, and glucose 10 (pH 7.4, osmolarity adjusted to 300 mosmol with sucrose, 21–24°C). After 40 min, the fura-2 containing solution was replaced by fresh HEPES-buffered saline and left for 15 min for de-esterification before commencing experiments. Fragments of coverslips were then placed in a perfusion chamber and $[Ca^{2+}]_i$ was measured using a Cairn Research ME-SE Photometry system (Cairn Research, Cambridge). Cells were superperfused (3–5 ml/min) under gravity and $[Ca^{2+}]_i$ was indicated by the ratio of fluorescence emitted at 510 nm due to alternating excitation at 340 nm and 380 nm using a monochromator. Drugs used to investigate Ca^{2+} homeostasis were applied to cells via switch of inflow chamber to one containing the HEPES-buffered saline and required drug. Ca^{2+}-free perfusate contained 1 m*M* EGTA and no added $CaCl_2$. The

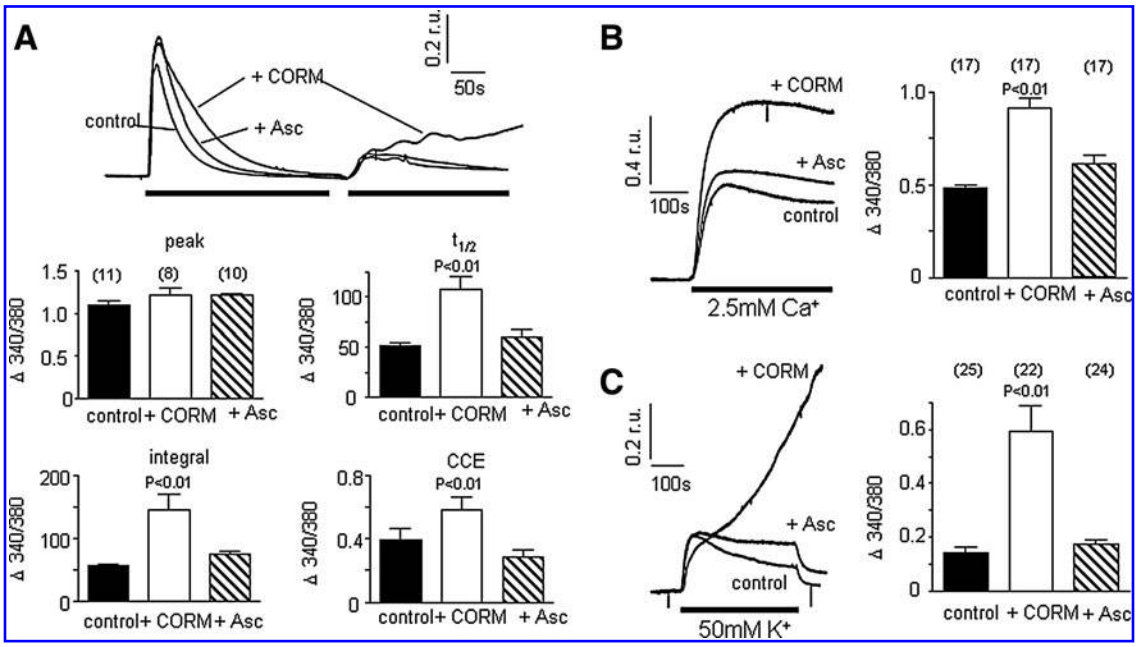

FIG. 6. The antioxidant ascorbic acid prevents the effects of CO. (A) Superimposed representative recordings of $[Ca^{2+}]_i$ made in SH-SY5Y cells in the absence (control) or presence of 30 μM CORM-2, and in the presence of both 30 μM CORM-2 and 200 μM ascorbic acid (+asc). Ca^{2+} was initially absent from the perfusate (replaced with 1 m*M* EGTA), and for the periods indicated by the *left-hand horizontal bar*, cells were exposed to 100 μM muscarine. Following washout of muscarine, Ca^{2+} was readmitted to the perfusate as indicated by the *right-hand bar*, and CCE determined. *Bar graphs* below plot mean responses to 100 μM muscarine evoked in the absence of other drugs (*solid bars*) in the presence of CORM-2 (30 μM; *open bars*) or in the presence of 30 μM CORM-2 and 200 μM ascorbic acid (*hatched bars*). Traces such as the ones shown above were measured for peak response (peak), the time taken for responses to fall to 50% of their peak value ($t_{1/2}$), and responses were also integrated (integral). The amplitudes of the CCE responses are also shown. In each case, *bars* represent means ± s.e.m., taken from the number of recordings indicated above each bar. *P* values indicate significant differences from controls. **(B)** *Left*, representative traces of capacitative Ca^{2+} entry (CCE) measured in cells in the absence (control) or presence of 10 μM of CORM-2 alone, or in the presence of 200 μM ascorbic acid (+asc.). Cells were previously exposed to 1 μM thapsigargin for 20 min in the absence of extracellular Ca^{2+}(replaced with 1 m*M* EGTA). Ca^{2+} (2.5 m*M*) was readmitted to the perfusate for the period indicated by the *horizontal bar*. *Right*, mean (± s.e.m.) peak CCE responses measured in control cells (*solid bar*), 10 μM CORM-2 (*open bars*) or 30 μM CORM-2 and 200 μM ascorbic acid. The number of recordings averaged are indicated above each bar. *P* values indicate significant differences from controls. **(C)** *Left*, representative recordings of $[Ca^{2+}]_i$ made in control cells, cells exposed to 30 μM CORM-2, and in the presence of both 30 μM CORM-2 and 200 μM ascorbic acid, as indicated. For the periods indicated by the bar, cells were exposed to perfusate containing 50 m*M* K^+. *Right*, mean (± s.e.m.) rises of $[Ca^{2+}]_i$ evoked by 50 m*M* K^+ in control cells (*solid bar*), 30 μM CORM-2 (*open bar*) and in the presence of both 30 μM CORM-2 and 200 μM ascorbic acid (*hatched bar*). The number of recordings averaged are indicated above each bar. *P* values indicate significant differences from controls.

high K^+ solution used in experiments was made by isotonic replacement of Na^+ in the perfusate (final $[K^+]$ 50 m*M*).

Electrophysiology

Fragments of coverslip with attached cells were transferred to a perfused (3–5 ml/min) recording chamber mounted on an Olympus CK40 inverted microscope. Whole cell patch clamp recordings were made using patch pipettes of 4–7 MΩ resistance. Series resistance was monitored after breaking into the whole cell configuration throughout the duration of experiments. If a significant increase occurred (>20%), the experiment was terminated. The perfusate (pH 7.4, NaOH; 22–24°C) was composed of (m*M*): NaCl (95); $MgCl_2$ (0.6); CsCl (5); HEPES (5); $BaCl_2$ (20); D-glucose (10); TEACl (20). The intracellular solution (pH 7.2, CsOH) consisted of (m*M*): CsCl (120); TEACl (20); EGTA (10); $MgCl_2$ (2); HEPES (10); MgATP (3); NaATP (2). CORM-2 was bath applied at the stated concentrations.

Signals were acquired using a Axopatch 200B controlled by Clampex 9.0 software via a Digidata 1322A interface (Axon Instruments, Inc., Foster City, CA). Data were filtered at 1 kHz and digitized at 2 kHz. To evoke ionic currents in SHSY5Y cells, a series of 100 ms depolarizing steps from −80 mV (holding potential) to +60 mV, in 10 mV increments, were employed. Offline analysis was carried out using the data analysis package Clampfit 9 (Axon Instruments) and data are expressed as mean ± SEM.

Monitoring NO production

DAF-FM was used to detect NO production fluorimetrically. Cells plated on coverslips were incubated with 5 m*M* DAF-FM (Invitrogen) in HEPES-buffered saline supplemented with 100 μM L-arginine and 0.002% pluronic acid for 40 min in the dark at room temperature. Thereafter the DAF-FM-containing solution was replaced by HEPES-buffered saline solution with 100 μM L-arginine in a perfusion chamber and NO was measured using a Cairn Research ME-SE Photometry system (Cairn Research, Cambridge). Cells were continuously superperfused under gravity and NO was

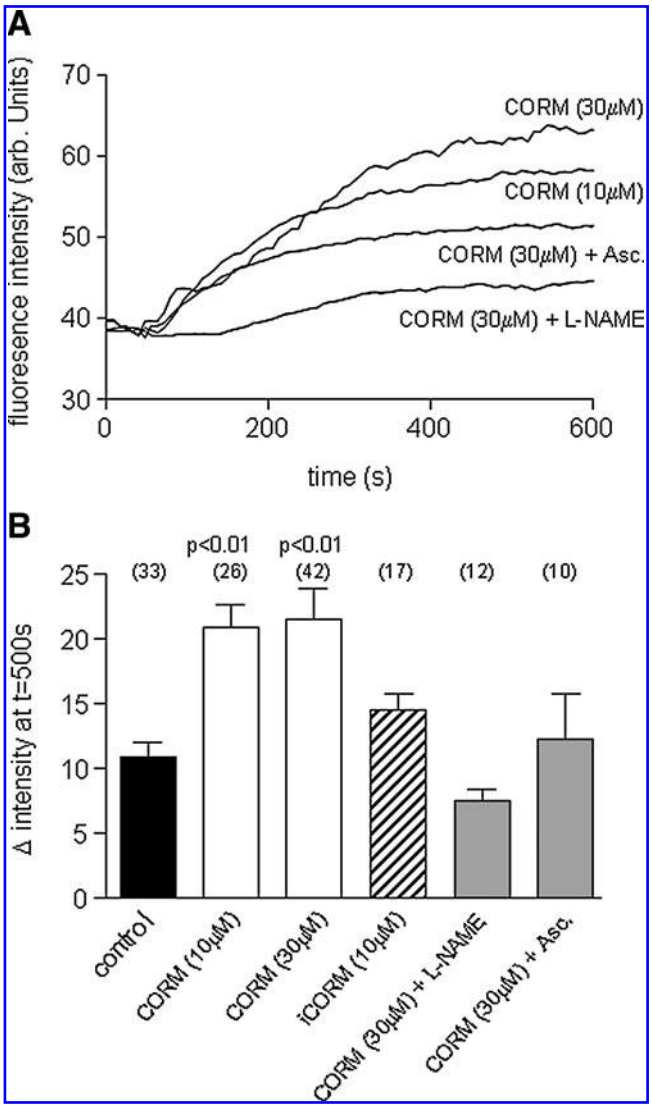

FIG. 7. CO stimulates $ONOO^-$ formation. (A) An example of recordings of APF fluorescence monitored in SH-SY5Y cells. At the point indicated by the *arrow*, cells were exposed to the drugs indicated. **(B)** Mean (±s.e.m., determined from the number of recordings indicated above each bar) APF fluorescence determined at $t = 510$ sec after exposure of cells to the drugs indicated. Control (*solid bar*) represents time-matched recordings where no drugs were added. *P* values indicate significant differences from controls.

indicated by the fluorescence emitted at 515 nm following excitation at 495 nm. In these experiments, the light path shutter was opened for 10 sec at 5 min intervals in order to avoid photobleaching of the dye.

Monitoring peroxynitrite production

Cells were plated on to coverslips in 24-well plates as before and incubated with 2- [6-(4'-amino)phenoxy-3H-xanthen-3-on-9-yl]benzoic acid (APF; 10 μM) dissolved in HEPES buffered saline in the dark for 1 h at 37°C. The coverslip was then cut into fragments and one fragment was placed on a glass slide containing 200 μl of HEPES buffered saline with 10 μM APF. APF was chosen both for its sensitivity to $ONOO^-$ and

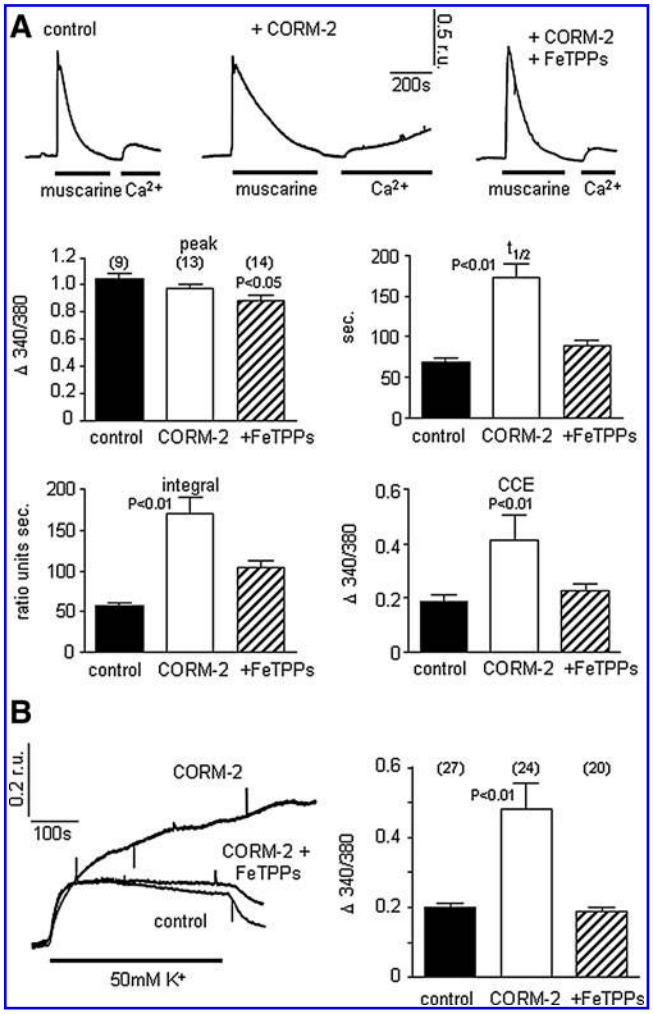

FIG. 8. Disruption of Ca^{2+} homeostasis by CO is dependent on $ONOO^-$ formation. (A) Representative recordings of $[Ca^{2+}]_i$ made in SH-SY5Y cells in the absence (control, *left*) or presence (*middle*) of 30 μM CORM-2, and in the presence of both 30 μM CORM-2 and 50 μM FeTPPS (*right*). In each case, Ca^{2+} was initially absent from the perfusate (replaced with 1 m*M* EGTA), and for the periods indicated by the *horizontal bars*, cells were exposed to 100 μM muscarine. Following washout of muscarine, Ca^{2+} was readmitted to the perfusate as indicated and CCE determined. *Bar graphs* plot mean responses to 100 μM muscarine evoked in the absence of other drugs (*solid bars*), in the presence of CORM-2 (30 μM; *open bars*), or in the presence of 30 μM CORM-2 and 50 μM FeTPPS (*hatched bars*). Traces such as the ones shown above were measured for peak response (peak), the time taken for responses to fall to 50% of their peak value ($t_{1/2}$) and responses were also integrated (integral). The amplitudes of the CCE responses are also shown. In each case, *bars* represent means±s.e.m., taken from the number of recordings indicated above each bar. *P* values indicate significant differences from controls. **(B)** *Left*, representative recordings of $[Ca^{2+}]_i$ made in control cells, cells exposed to 30 μM CORM-2, and in the presence of both 30 μM CORM-2 and 50 μM FeTPPS, as indicated. For the periods indicated by the *bar*, cells were exposed to perfusate containing 50 m*M* K^+. *Right*, mean (±s.e.m.) rises of $[Ca^{2+}]_i$ evoked by 50 m*M* K^+ in control cells (*solid bar*), 30 μM CORM-2 (*open bar*), and in the presence of both 30 μM CORM-2 and 50 μM FeTPPS (*hatched bar*). The number of recordings averaged are indicated above each bar. *P* value indicates significant difference from controls.

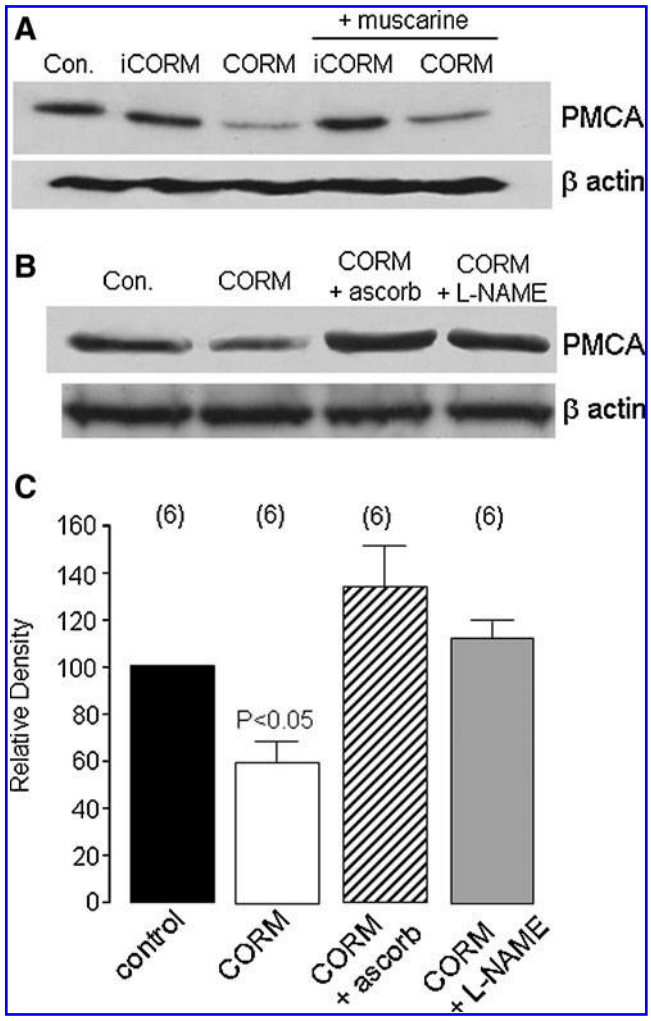

FIG. 9. CO causes loss of PMCA in SH-SY5Y cells. (A) Western blot showing the effects of the CO donor CORM-2 (30 μM) and iCORM (30 μM) on plasmalemmal Ca^{2+} ATPase (PMCA) protein levels in the absence and presence of muscarine (100 μM). *Lower blot* shows β actin loading controls. **(B)** Western blot exemplifying the restoration of PMCA levels by ascorbic acid (200 μM) or L-NAME (1 μM) when applied simultaneously with CORM-2 (30 μM) for 20 min. *Lower blot* shows b actin loading controls. **(C)** Mean (±s.e.m., taken from the number of experiments indicated above each bar) densitometric measurements of PMCA protein levels under the conditions indicated. *P* value indicates significant difference from controls.

for relative insensitivity to O_2^- and also because it is resistance to light-induced auto-oxidation. Changes in fluorescence intensity were measured over 10 min using a ZEISS (Oberkochen, Germany) laser scanning confocal microscope (LSM 510). The fluorophore was excited at 488 nm and emission monitored at 510 nm. Zeiss AIM software was used to obtain the images. Identical settings were used for each test condition. For APF experiments with L-NAME, the cells were incubated with both 10 μM APF and 1 mM L-NAME for 1h at 37°C prior to starting the recordings.

Western blot analysis

Cells were grown to near confluence in 25 cm^2 flasks, treated with test substance as indicated, washed with PBS,

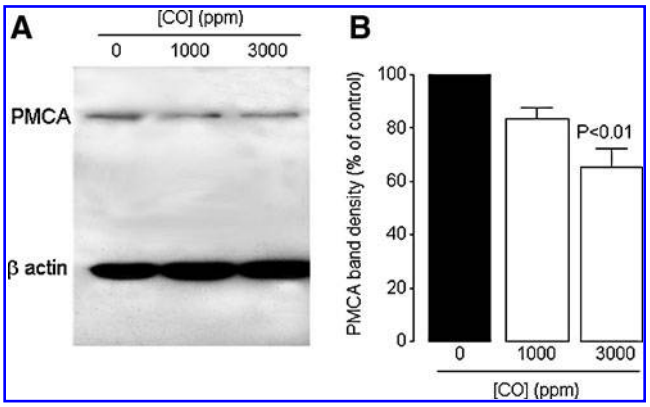

FIG. 10. CO inhalation causes loss of brain PMCA *in vivo*. (A) Western blot showing the effects of the CO inhalation (1000 and 3000 ppm) on plasmalemmal Ca^{2+} ATPase (PMCA) protein levels in whole rat brain homogenates. **(B)** Mean (±s.e.m., $n=4$ animals) densitometric measurements of PMCA protein levels under the conditions indicated. *P* value indicates significant difference from controls.

and then solubilized *in situ* in 300 μl mammalian protein extraction reagent (Pierce Perbio, UK) containing a Complete mini-protease inhibitor tablet (Roche Bioscience, UK). Cell proteins (20 mg protein per lane) were separated on 7.5%, 0.75 mm polyacrylamide SDS gels and electrophoretically transferred to PVDF membranes (BioRad). Blots were incubated in 5% non-fat milk protein and then probed with a monoclonal antibody raised against plasma membrane Ca^{2+} ATPases (1:100; PMCA (H8); Santa Cruz Biotechnology Inc, Santa Cruz, CA). Bands were visualized using an enhanced chemiluminescence detection system (ECL) and hyperfilm ECL (GE Healthcare, UK). Approximate equal loading of proteins was confirmed by blotting with monoclonal β-actin antibody (1/2000, Sigma) in 5% non-fat milk protein in TBS. Band densities were measured using ImageJ and expressed as a percentage of the control (untreated) band density.

In vivo *CO exposure*

Male Sprague-Dawley rats (260–280 g) were individually put in a plastic chamber (26.5 cm in diameter, 28.5 cm in height) and exposed to 1000 or 3000 ppm CO for 40 min, as previously reported (16). After reoxygenation for 2 h, the brain was removed under pentobarbital anesthesia (50 mg/kg, i.p.) and immediately frozen on dry ice. The control rats were exposed to room air alone for 40 min. Brain cortices were homogenized in ice-cold RIPA buffer containing a complete mini-protease inhibitor tablet (Roche Bioscience, UK) at 3 ml per gram of tissue, disrupted by sonication, and incubated on ice for 30 min. Crude homogenates were then cleared by centrifugation (10,000 *g* 10 min). The supernatant was removed and centrifuged (15,000 *g* 15 min) again, and the total cell lysate removed and immediately frozen in liquid N_2. The cleared brain homogenates were probed by Western blots as described above.

Drugs and dyes employed

The following compounds were employed in this study, as described in the Results section. Muscarine, CORM-2, L-NAME, thapsigargin, ascorbic acid, antimycin A and APF

were all obtained from Sigma Aldrich. Cyclopiazonic acid (CPA) and S-nitroso N-acetylpenicillamine (SNAP) were from Ascent Scientific. DEA NONOate and DPTA NONOate were from Cayman Chemicals. The NO donor, s-nitrosocysteine, was synthesized in-house immediately before use in experiments, as described by (5). Fura-2AM and DAF-FM were from Invitrogen, Fe-TPPS from Calbiochem.

Statistical analysis

Data are presented as individual examples and analyzed results presented as mean ± SEM. Statistical analysis was carried out using one way ANOVA followed by a post hoc test unless indicated otherwise. *P* values of less than 0.05 were considered significant.

Acknowledgment

This work was supported by the Alzheimer's Society, UK.

Disclosure Statement

None of the authors have any conflicts to disclose regarding this submission.

References

1. Ahmad AS, Zhuang H, and Dore S. Heme oxygenase-1 protects brain from acute excitotoxicity. *Neuroscience* 141: 1703–1708, 2006.
2. Bezprozvanny I and Mattson MP. Neuronal calcium mishandling and the pathogenesis of Alzheimer's disease. *Trends Neurosci* 31: 454–463, 2008.
3. Bilban M, Haschemi A, Wegiel B, Chin BY, Wagner O, and Otterbein LE. Heme oxygenase and carbon monoxide initiate homeostatic signalling. *J Mol Med* 86: 267–279, 2008.
4. Brini M and Carafoli E. Calcium pumps in health and disease. *Physiol Rev* 89: 1341–1378, 2009.
5. Burgoyne JR and Eaton P. A rapid approach for the detection, quantification, and discovery of novel sulfenic acid or S-nitrosothiol modified proteins using a biotin-switch method. *Methods Enzymol* 473: 281–303, 2010.
6. Choi S, Kim JH, Roh EJ, Ko MJ, Jung JE, and Kim HJ. Nuclear factor-kappaB activated by capacitative Ca2+ entry enhances muscarinic receptor-mediated soluble amyloid precursor protein (sAPPalpha) release in SH-SY5Y cells. *J Biol Chem* 281: 12722–12728, 2006.
7. Cobb N and Etzel RA. Unintentional carbon monoxide-related deaths in the United States, 1979 through 1988. *JAMA* 266: 659–663, 1991.
8. Gandini C, Castoldi AF, Candura SM, Locatelli C, Butera R, Priori S, and Manzo L. Carbon monoxide cardiotoxicity. *J Toxicol Clin Toxicol* 39: 35–44, 2001.
9. Gorman D, Drewry A, Huang YL, and Sames C. The clinical toxicology of carbon monoxide. *Toxicology* 187: 25–38, 2003.
10. Gozzelino R, Jeney V, and Soares MP. Mechanisms of cell protection by heme oxygenase-1. *Annu Rev Pharmacol Toxicol* 50: 323–354, 2010.
11. Green KN and LaFerla FM. Linking calcium to Abeta and Alzheimer's disease. *Neuron* 59: 190–194, 2008.
12. Guan L, Wen T, Zhang Y, Wang X, and Zhao J. Induction of heme oxygenase-1 with hemin attenuates hippocampal injury in rats after acute carbon monoxide poisoning. *Toxicology* 262: 146–152, 2009.
13. Gutierrez-Martin Y, Martin-Romero FJ, Henao F, and Gutierrez-Merino C. Synaptosomal plasma membrane Ca(2+) pump activity inhibition by repetitive micromolar ONOO(-) pulses. *Free Radic Biol Med* 32: 46–55, 2002.
14. Haldane J. The relation of the action of carbonic oxide to oxygen tension. *J Physiol* 18: 201—217, 1895.
15. Halliwell B and Gutteridge JMC. *Free Radicals in Biology and Medicine.* Oxford, UK, Oxford University Press, 2007, p. 61.
16. Hara S, Mizukami H, Mukai T, Kurosaki K, Kuriiwa F, and Endo T. Involvement of extracellular ascorbate and iron in hydroxyl radical generation in rat striatum in carbon monoxide poisoning. *Toxicology* 264: 69–73, 2009.
17. Harper A and Croft-Baker J. Carbon monoxide poisoning: Undetected by both patients and their doctors. *Age Ageing* 33: 105–109, 2004.
18. Hettiarachchi NT, Parker A, Dallas ML, Pennington K, Hung CC, Pearson HA, Boyle JP, Robinson P, and Peers C. alpha-Synuclein modulation of Ca2+ signaling in human neuroblastoma (SH-SY5Y) cells. *J Neurochem* 111: 1192–1201, 2009.
19. Kim HP, Ryter SW, and Choi AM. CO as a cellular signaling molecule. *Annu Rev Pharmacol Toxicol* 46: 411–449, 2006.
20. Kruman II and Mattson MP. Pivotal role of mitochondrial calcium uptake in neural cell apoptosis and necrosis. *J Neurochem* 72: 529–540, 1999.
21. Lim I, Gibbons SJ, Lyford GL, Miller SM, Strege PR, Sarr MG, Chatterjee S, Szurszewski JH, Shah VH, and Farrugia G. Carbon monoxide activates human intestinal smooth muscle L-type Ca2+ channels through a nitric oxide-dependent mechanism. *Am J Physiol Gastrointest Liver Physiol* 288: G7–14, 2005.
22. Mannaioni PF, Vannacci A, and Masini E. Carbon monoxide: The bad and the good side of the coin, from neuronal death to anti-inflammatory activity. *Inflamm Res* 55: 261–273, 2006.
23. Mattson MP. Neuronal life-and-death signaling, apoptosis, and neurodegenerative disorders. *Antioxid Redox Signal* 8: 1997–2006, 2006.
24. Mattson MP. Calcium and neurodegeneration. *Aging Cell* 6: 337-350, 2007.
25. Meredith T and Vale A. Carbon monoxide poisoning. *Br Med J (Clin Res Ed)* 296: 77–79, 1988.
26. Min SK. A brain syndrome associated with delayed neuropsychiatric sequelae following acute carbon monoxide intoxication. *Acta Psychiatr Scand* 73: 80–86, 1986.
27. Misko TP, Highkin MK, Veenhuizen AW, Manning PT, Stern MK, Currie MG, and Salvemini D. Characterization of the cytoprotective action of peroxynitrite decomposition catalysts. *J Biol Chem* 273: 15646–15653, 1998.
28. Morton AJ, Hammond C, Mason WT, and Henderson G. Characterisation of the L- and N-type calcium channels in differentiated SH-SY5Y neuroblastoma cells: Calcium imaging and single channel recording. *Brain Res Mol Brain Res* 13: 53–61, 1992.
29. Motterlini R and Otterbein LE. The therapeutic potential of carbon monoxide. *Nat Rev Drug Discov* 9: 728–743, 2010.
30. Nelson CP, Nahorski SR, and Challiss RA. Temporal profiling of changes in phosphatidylinositol 4,5-bisphosphate, inositol 1,4,5-trisphosphate and diacylglycerol allows comprehensive analysis of phospholipase C-initiated signaling in single neurons. *J Neurochem* 107: 602–615, 2008.
31. Piantadosi CA. Carbon monoxide, reactive oxygen signaling, and oxidative stress. *Free Radic Biol Med* 45: 562–569, 2008.
32. Prockop LD and Chichkova RI. Carbon monoxide intoxication: An updated review. *J Neurol Sci* 262: 122–130, 2007.
33. Purkiss JR, Nahorski SR, and Willars GB. Mobilization of inositol 1,4,5-trisphosphate-sensitive Ca2+ stores supports

bradykinin- and muscarinic-evoked release of [3H] noradrenaline from SH-SY5Y cells. *J Neurochem* 64: 1175–1182, 1995.
34. Rana B, Mcmorn SO, Reeve HL, Wyatt CN, Vaughan PFT, and Peers C. Inhibition of neuronal nicotinic acetylcholine-receptors by imipramine and desipramine. *Eur J Pharmacol* 250: 247–251, 1993.
35. Reeve HL, Vaughan PFT, and Peers C. Calcium-channel currents in undifferentiated human neuroblastoma (sh- sy5y) cells. Actions and possible interactions of dihydropyridines and omega-conotoxin. *Eur J Neurosci* 6: 943–952, 1994.
36. Ryter SW and Choi AM. Heme oxygenase-1/carbon monoxide: From metabolism to molecular therapy. *Am J Respir Cell Mol Biol* 41: 251–260, 2009.
37. Saito S, Yamamoto-Katou A, Yoshioka H, Doke N, and Kawakita K. Peroxynitrite generation and tyrosine nitration in defense responses in tobacco BY-2 cells. *Plant Cell Physiol* 47: 689–697, 2006.
38. Setsukinai K, Urano Y, Kakinuma K, Majima HJ, and Nagano T. Development of novel fluorescence probes that can reliably detect reactive oxygen species and distinguish specific species. *J Biol Chem* 278: 3170–3175, 2003.
39. Smith IF, Boyle JP, Vaughan PF, Pearson HA, Cowburn RF, and Peers CS. Ca^{2+} stores and capacitative Ca^{2+} entry in human neuroblastoma (SH-SY5Y) cells expressing a familial Alzheimer's disease presenilin-1 mutation. *Brain Res* 949: 105–111, 2002.
40. Smith IF, Boyle JP, Vaughan PF, Pearson HA, and Peers C. Effects of chronic hypoxia on Ca^{2+} stores and capacitative Ca^{2+} entry in human neuroblastoma (SH-SY5Y) cells. *J Neurochem* 79: 877–884, 2001.
41. Soares MP, Usheva A, Brouard S, Berberat PO, Gunther L, Tobiasch E, and Bach FH. Modulation of endothelial cell apoptosis by heme oxygenase-1-derived carbon monoxide. *Antioxid Redox Signal* 4: 321–329, 2002.
42. Stoller KP. Hyperbaric oxygen and carbon monoxide poisoning: A critical review. *Neurol Res* 29: 146–155, 2007.
43. Thom SR, Fisher D, Xu YA, Notarfrancesco K, and Ischiropoulos H. Adaptive responses and apoptosis in endothelial cells exposed to carbon monoxide. *Proc Natl Acad Sci USA* 97: 1305–1310, 2000.
44. Thom SR, Fisher D, Zhang J, Bhopale VM, Cameron B, and Buerk DG. Neuronal nitric oxide synthase and N-methyl-D-aspartate neurons in experimental carbon monoxide poisoning. *Toxicol Appl Pharmacol* 194: 280–295, 2004.
45. Thom SR, Xu YA, and Ischiropoulos H. Vascular endothelial cells generate peroxynitrite in response to carbon monoxide exposure. *Chem Res Toxicol* 10: 1023–1031, 1997.
46. Vaughan PFT, Peers C, and Walker JH. The use of the human neuroblastoma SH-SY5Y to study the effect of 2nd-messengers on noradrenaline release. *Gen Pharmacol* 26: 1191–1201, 1995.
47. Vieira HL, Queiroga CS, and Alves PM. Pre-conditioning induced by carbon monoxide provides neuronal protection against apoptosis. *J Neurochem* 107: 375–384, 2008.
48. Von Burg R. Carbon monoxide *J Appl Toxicol* 19: 379–386, 1999.
49. Zeynalov E and Dore S. Low doses of carbon monoxide protect against experimental focal brain ischemia. *Neurotox Res* 15: 133–137, 2009.
50. Zuckerbraun BS, Chin BY, Bilban M, de Costa dJ, Rao J, Billiar TR, and Otterbein LE. Carbon monoxide signals via inhibition of cytochrome c oxidase and generation of mitochondrial reactive oxygen species. *FASEB J* 21: 1099–1106, 2007.

Address correspondence to:
Prof. Chris Peers
Division of Cardiovascular and Neuronal Remodelling
Leeds Institute of Genetics, Health, and Therapeutics
Worsley Building, Level 10
University of Leeds
Leeds LS2 9JT
United Kingdom

E-mail: c.s.peers@leeds.ac.uk

Date of first submission to ARS Central, November 4, 2011; date of final revised submission, January 23, 2012; date of acceptance, February 22, 2012.

Abbreviations Used

APF = 2-[6-(4′-amino)phenoxy-3H-xanthen-3-on-9-yl]benzoic acid
CCE = capacitative Ca^{2+} entry
CORM-2 = carbon monoxide releasing molecule
CPA = cyclopiazonic acid
CysNO = S-nitrosocysteine
DAF 2 = 4,5-diaminofluorescein
DEA NONOate = diethylammonium (Z)-1-(N,N-diethylamino)diazen-1-ium-1,2-diolate
DPTA NONOate = (Z)-1-[N-(3-aminopropyl)-N-(3-ammoniopropyl)amino]diazen-1-ium-1,2-diolate
EGTA = ethylene glycol-bis(2-aminoethylether)-*N,N,N′,N′*-tetraacetic acid
FeTPPS = 5,10,15,20-tetrakis-[4-sulfonatophenyl]-porphyrinato-iron[III]
iCORM = inactive carbon monoxide releasing molecule
IP_3 = inositol trisphosphate
L-NAME = *N*-Nitro-L-arginine methyl ester
PMCA = plasma membrane Ca^{2+}ATPase
RO = reactive oxygen species
SNAP = S-nitroso N-acetylpenicillamine
TG = thapsigargin